Stable Low-Temperature Photoproducts and Hole Burning of Green Fluorescent Protein (GFP)

C. Seebacher, F. W. Deeg,* and C. Bräuchle*

Institut für Physikalische Chemie, Ludwig-Maximilians-Universität München, Butenandtstrasse 5-13 E, 81377 München, Germany

J. Wiehler and B. Steipe

Genzentrum der Ludwig-Maximilians-Universität München, Feodor-Lynen-Strasse 25, 81377 München, Germany

Received: March 12, 1999; In Final Form: June 14, 1999

We present low-temperature optical investigations down to 2 K of the photochemistry and hole burning of wild-type green fluorescent protein (wt-GFP). Three new photoproducts with absorption at 489, 502, and 510 nm (P489, P502, P510, respectively) are identified by fluorescence excitation and fluorescence spectroscopy. The data suggest that P502 is identical with the obligatory intermediate of the excited-state deprotonation cycle R^-_{neq} that exists only as a transient at room temperature. The second new product P510 is also associated with R^-_{neq}, whereas P489 is related to the equilibrated anionic form R^-_{eq}. An extended energy scheme accounting for these new species is presented. The ground-state energy barriers characterizing these products have been determined by temperature-dependent studies. Low-temperature persistent spectral hole burning in the red wing of the R^-_{eq} absorption has been demonstrated and can be used to characterize electron−phonon coupling.

1. Introduction

The green fluorescent protein (GFP)[1] of the jellyfish *Aequorea victoria* exhibits a strong green fluorescence if illuminated with blue light. No exogenous fluorophore is required as an autocatalytic cyclization and oxidation of an internal tripeptide unit forms the fluorophore. The protein consists of 238 amino acids which form a structure that has been called a β-can, with the fluorophore packed inside.[2] It is known that the chromophore exists in two stable forms. Excitation and fluorescence spectra have been recorded by Chattoraj et al.[3] and Lossau et al.[4] They show a strong absorption at 471 nm with structured vibronic bands at low-temperature associated with an anionic form R^-_{eq}, and a broad unstructured absorption band around 404 nm originating from a protonated form RH. Although the two forms can easily be distinguished in their absorption, they fluoresce at similar wavelengths, due to an excited-state proton transfer of RH. The ratio between these two forms is dependent on the pH and the solvent.[4] A generic energy scheme summarizing these results is shown in Figure 1.

Due to its intrinsic fluorophore, GFP has found widespread use as a label in biophysical and biochemical investigations.[5,6] It has been demonstrated recently that with a sensitive fluorescence apparatus even individual GFP molecules can be detected and monitored at room temperature.[7,8] Single molecule spectroscopy allows gathering information about the characteristics of local environments unobserved by ensemble averaging.

For these reasons a detailed knowledge of the structure and dynamics of GFP is of utmost interest. In this paper we will present the first investigation of GFP at temperatures below 77 K. The main goal is a detailed characterization of the electronic energy surface of GFP. More specifically we want to present information about new substates, energy barriers, and relaxation pathways. Conformations of the protein which are only transiently populated at high temperature can be frozen out at low temperature. In addition, at liquid helium temperature optical high resolution techniques like fluorescence line narrowing and spectral hole burning allow us to select subensembles within the inhomogeneously broadened absorption band. In this way variations in the local environment of the chromophore can be resolved and contributions to the heterogeneity can be characterized.[9]

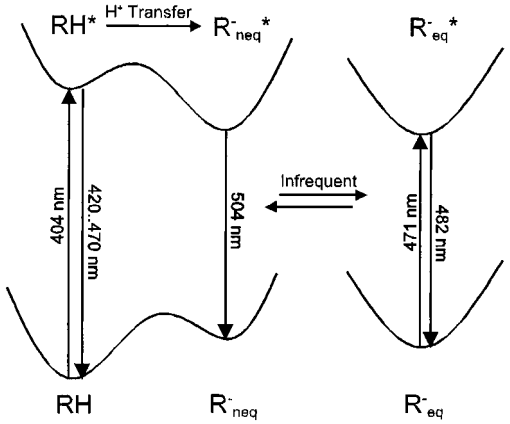

Figure 1. Simplified low-temperature energy scheme of wt-GFP showing the excited-state proton transfer and bleaching into an equilibrated state of the anion. The indicated wavelengths refer to data taken at 77 K.[3] Data in the literature[3,4] differ slightly, probably because of different temperatures and solvents used.

2. Experimental Section

In this paper only investigations of wt-GFP will be reported. wt-GFP used in this study was based on the *Aequorea victoria*

* Authors to whom correspondence should be addressed.

10.1021/jp990883k CCC: $18.00
Published on Web 08/13/1999

gene[5] containing the Gln80Arg mutation. To prepare the gene for expression and purification, its NcoI restriction site was eliminated. Then a novel Nco I site overlapping with the initiation ATG at the 5′-end and a Bst EII site at the 5′-end was introduced. Deviating from the published sequence, the N-terminal Ser2 was changed to Gly and another Gly was appended to the C-terminus. The gene was cloned into plasmid pRSET 5d resulting in the expression plasmid pT7GFPav. Expression is under control of the T7 promoter and one-step purification of the expressed protein is possible via a C-terminal His6 tag. The protein was expressed in *E. coli* BL21(-DE3) at 25 °C. Expression was induced with 0.5 mM IPTG and cells harvested after 4 h. The soluble cytoplasmic fraction was applied to a Ni-NTA Agarose column (Quiagen). Columns were washed with 6−8 volumes of 40 mM imidazole, 300 mM NaCl, 50 mM Na_2HPO_4 (pH 7.0), and eluted with ∼3 column volumes of buffer by increasing the imidazole concentration to 0.5 M. SDS−PAGE of the pooled eluate indicated a purity greater than 99%. Final yields were ∼10 mg of purified protein per liter of culture. The sample was diluted to a concentration of ca. 10^{-6} mol/L with a 70% glycerol:30% aqueous phosphate buffer mixture (pH = 7) and filled in a 1 mm thick sample cell (Vitrodynamics).

The sample was cooled in a flow cryosystem (Cryovac) down to 2 K and temperature-controlled with a PID-regulator (LakeShore 330). A Xe arc lamp (Oriel 66002), dispersed by a double monochromator (Spex 1402) with a resolution of 0.03 nm, was used for the fluorescence excitation spectra. The fluorescence was passed through a long-pass optical filter (OG550, Schott) and detected with a GaAs photomultiplier (C30034, Hamamatsu) and a photon counting system (SR400/440, Stanford Research). To correct the spectra for the characteristics of the arc lamp, all spectra were divided by the lamp spectrum recorded with the same system.

The fluorescence spectra were obtained by illumination with various selected lines from an Ar or Kr ion laser source (Coherent) and detected with the double monochromator and the photon counting system. Laser illumination for photochemistry was done with the same wavelengths and setup as the fluorescence spectra.

3. Results

3.1. Excitation Spectroscopy. Figure 2 shows the fluorescence excitation spectra of wt-GFP at 2 K under various illumination conditions. The spectrum of wt-GFP before any laser illumination is shown at the top (A). It is very similar to the excitation spectrum at 77 K reported in the literature.[3] In contrast to the room-temperature spectrum these low-temperature spectra exhibit a structured band of R^-_{eq} which persists up to 200 K. The long wavelength absorption band has a maximum at 471 nm and is Gaussian shaped with a width (fwhm) of approximately 12 nm. This line broadens slightly with increasing temperature. Vibrational transitions at 460 nm ($\Delta\tilde{\nu} = 500$ cm^{-1}) and 446 nm ($\Delta\tilde{\nu} = 1200$ cm^{-1}) couple to the electronic transition.[3,4]

Upon illumination of the sample with an Ar ion laser at λ_{ex} = 472.7 nm (100 mW/cm^2, 60 min) the absorption band due to the anionic form of the chromophore decreases while a photoproduct P489 with an absorption maximum at 489 nm develops (Figure 2B). The excitation spectra are normalized to the isosbestic point found at 477.5 nm. Illumination of the wt-GFP sample in the protonated form at 363.8 nm (30 mW/cm^2, 240 min) induces a new product P502 with an absorption maximum at 502 nm and a third product P510 with an absorption band at 510 nm as shown in Figure 2C. P502 and P510 are also generated if the sample is illuminated with λ_{ex} = 406.7 nm. However, in contrast to illumination at 363.8 nm under these conditions a considerable amount of P489 is produced, too, due to the overlap of the absorption bands of RH and R^-_{eq}.

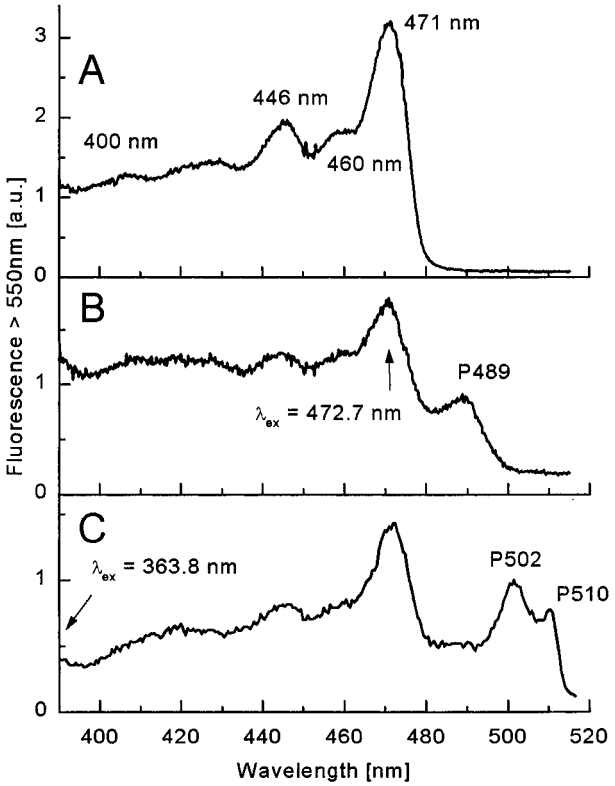

Figure 2. Fluorescence excitation spectra of wt-GFP in 70% glycerol: 30% aqueous buffer (pH = 7) at 2 K. All spectra depicted in this paper are taken on the same sample. All excitation spectra are recorded with a fluorescence long-pass filter >550 nm. (A) Spectrum before illumination, (B) spectrum after illumination with λ_{ex} = 472.7 nm (100 mW/cm^2 for 60 min), (C) spectrum after illumination with λ_{ex} = 363.8 nm (30 mW/cm^2, 240 min).

3.2. Fluorescence Spectroscopy. Fluorescence spectroscopy was used to gain further information about the new photoproducts. Fluorescence spectra of wt-GFP and the low-temperature photoproducts together with the respective fluorescence excitation spectra (dotted) are shown in Figure 3. The top spectra (A) show the fluorescence of the protonated wt-GFP chromophore RH (excited at 363.8 nm) with a maximum at 503 nm as well as that of the deprotonated chromophore R^-_{eq} (excited at 472.7 nm) with a maximum at 482 nm. RH has a large spectral shift of about 100 nm due to the excited-state deprotonation. R^-_{eq} exhibits a Stokes shift of 9 nm (472.7 nm → 482 nm), an order of magnitude smaller than in the protonated chromophore. The fluorescence spectra of wt-GFP as well as of all photoproducts (see below) show a weak vibronic band at $\Delta\tilde{\nu} = 500$ cm^{-1} and a strong vibronic band at $\Delta\tilde{\nu} = 1400$ cm^{-1} with respect to the 0−0 transition. A weak broad band between 420 and 470 nm has been attributed to the fluorescence of RH*.[3,4]

The fluorescence spectra associated with the new low-temperature excitation bands are depicted in Figures 3B−D. All low-temperature photoproducts show a rather small Stokes shift. Exciting P489 with a 488.0 nm Ar ion laser results in a fluorescence maximum at 496 nm (see Figure 3B). P502 can be excited with the 501.7 nm Ar ion laser line and shows a fluorescence maximum at 505 nm with a weak shoulder at 511

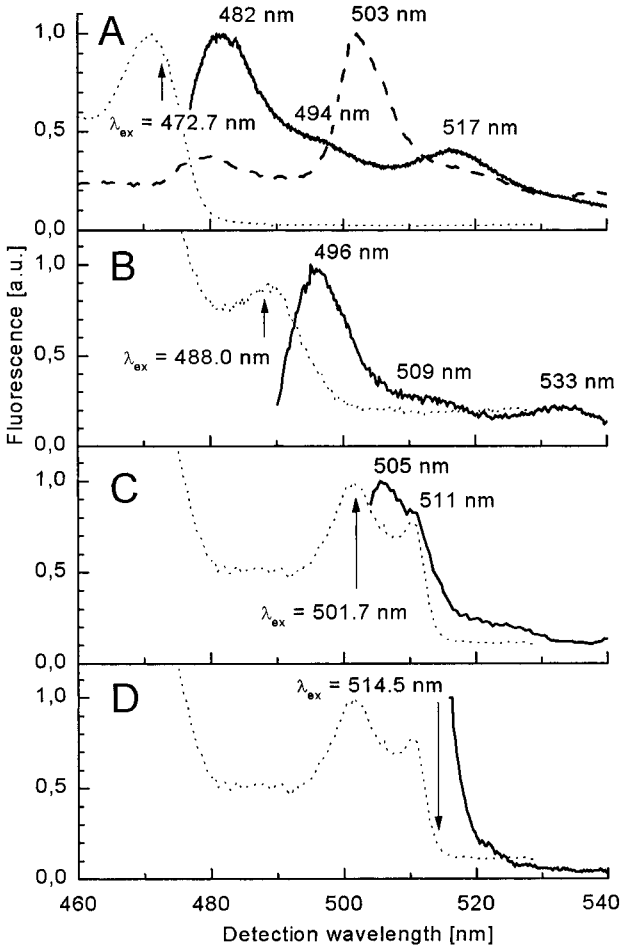

Figure 3. Fluorescence spectra of wt-GFP and the low-temperature photoproducts together with the respective excitation spectra detected above 550 nm (dotted), arrows indicate respective excitation wavelength. (A) Fluorescence of R^-_{eq} (solid line, $\lambda_{ex} = 472.7$ nm) and RH (dashed line, $\lambda_{ex} = 363.8$ nm, excitation wavelength outside depicted range), (B) fluorescence of P489 ($\lambda_{ex} = 488.0$ nm), (C) fluorescence of P502 ($\lambda_{ex} = 501.7$ nm), (D) fluorescence of P510 ($\lambda_{ex} = 514.5$ nm).

nm (see Figure 3C). This shoulder is attributed to the fluorescence of P510, which weakly absorbs at 501.7 nm. As no suitable laser line for excitation of P510 was available, this photoproduct was illuminated in the far-red wing of the band with the 514.5 nm Ar ion laser line. No fluorescence maximum can be resolved under these circumstances. On the basis of the observations in Figure 3C,D we conclude that the Stokes shift of P510 is below 1 nm. The vibrational structure of the fluorescence spectra in Figure 3B,C is similar to the one in the fluorescence spectrum of the anionic chromophore in Figure 3A (the dominant vibronic band in Figure 3C at 544 nm is outside of the wavelength range shown).

Selective excitation within the inhomogeneously broadened band is possible. Excitation at 472.7 nm leads to a fluorescence maximum at 481 nm while excitation at 476.5 and 482.5 nm results in shifted fluorescence spectra with maxima at 484 and 490 nm, respectively (not shown here). However, no fluorescence line narrowing is observed.

3.3. Persistent Spectral Hole Burning. We have also tested the feasibility of burning persistent spectral holes at low temperature in this system. Figure 4 shows a hole burnt with a Kr ion laser at 482.5 nm in the far-red wing of the absorption band of R^-_{neq} and detected through fluorescence excitation. The normalized spectrum shows a narrow hole with a line width limited by the monochromator resolution of 0.03 nm. The

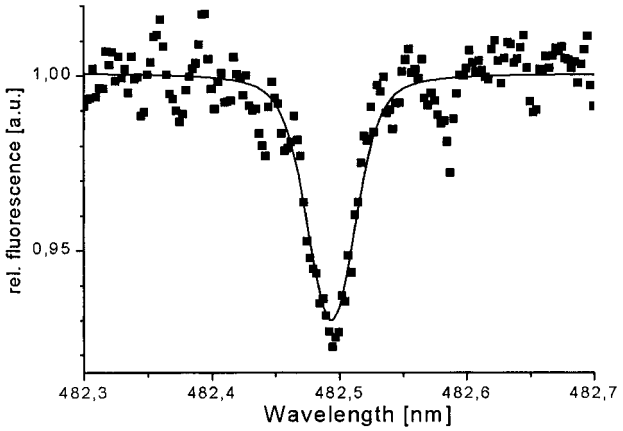

Figure 4. Spectral hole burnt in wt-GFP. The persistent spectral hole was burnt with a Kr ion laser at 482.5 nm with 16 mW/cm^2 for 30 min at 2 K. The measured hole width of 0.03 nm is limited by the resolution of the monochromator.

spectral hole is stable at temperatures at and below 25 K. We assume that the burning mechanism is identical to the photochemical transformation described above. A detailed investigation of the product bands following hole burning is under way.

3.4. Temperature Dependence of Spectra. To gather more information about the new photoproducts in this investigation, more specifically the ground state energy barriers associated with them, we have performed temperature-dependent experiments. After generation of the photoproduct at $T = 2$ K, as described above, the sample was slowly heated, thereby promoting conversion and loss of the initial photoproduct, which was monitored by the loss of fluorescence from the species. In this way, the energy barriers for interconversion of the ground-state species can be measured. Under the experimental conditions the fluorescence intensity at a given temperature is constant on the time scale of the experiment.

Figure 5A shows the change of fluorescence from the various low-temperature photoproducts upon increasing the temperature of the sample. For the P489 and the P502 species the sample was illuminated with 488.0 and 501.7 nm, respectively, while the fluorescence was detected at 496 and 510 nm, respectively. The P510 photoproduct was illuminated at 510 nm from a Xe arc lamp while the fluorescence was detected with a long-pass optical filter OG550.

As shown in Figure 5A the three photoproducts disappear at different temperature. P510 disappears at about 50 K, P502 is stable up to 90 K, while P489 vanishes at about 130 K. As will be shown in detail in the Discussion Section, one can derive the distribution of energy barriers for the various photoproducts by taking the derivatives of the curves in Figure 5A with respect to temperature. These derivated curves are shown in Figure 5B.

4. Discussion

All three new low-temperature photoproducts absorb around 500 nm. As the protonated chromophore emits at 420−470 nm, we therefore assume that they all contain a deprotonated chromophore. The large spectral shift of the protonated chromophore RH is due to excited-state deprotonation into R^-_{neq} followed by reorganization and emission. We demonstrate that excited-state deprotonation even at 2 K is possible. Illumination of R^-_{eq} produces only P489. Excitation at lower wavelengths, where RH (the starting point of the excited state proton transfer) dominates the absorption, leads to P502 and P510 as the main photoproducts. The emission of P502 is virtually identical to the emission of the chromophore after excitation at 363.8 nm.

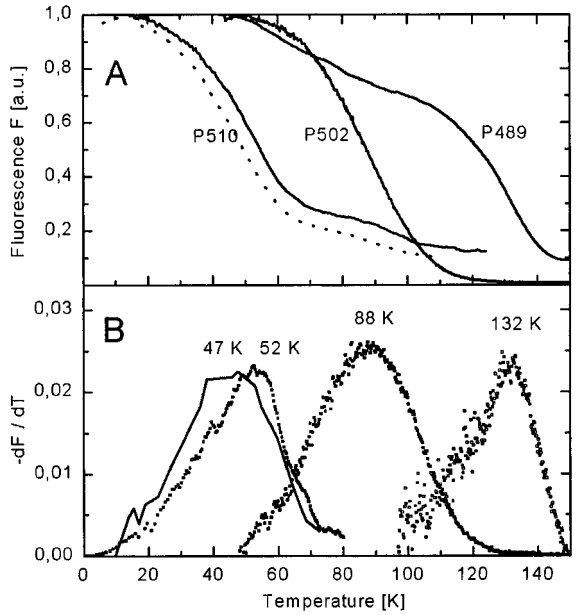

Figure 5. (A) Change of fluorescence of the three photoproducts upon sample heating. The dotted line has been recorded with a heating rate of 10 K per 3000 s; the three other curves were measured with a heating rate of 10 K per 70 s. (B) Negative derivatives of the curves above. These curves represent the barrier distribution associated with the various photoproducts. The temperatures listed are the respective values of the maxima of the curves.

We suggest that P502 is actually identical to R^-_{neq}. This implies that the obligatory intermediate, which has a lifetime below 1 ns at room temperature,[4] is stable at 2 K and thus can be spectroscopically characterized in detail.

The new low-temperature species P510 is generated by illuminating RH as is P502. However, as obvious from Figure 5, P510 disappears at a much lower temperature than P502. This proves that the band at 510 nm cannot be a vibronic band associated with P502 but has to be attributed to an independent photoproduct.

We have not observed photoconversion between RH and R^-_{eq} at 2 K, which is consistent with the fact that the conversion is already slow at room temperature.[3,7] The activation barrier for this process must be much higher than the thermal energy available to the molecule at a temperature of 2 K. As P489 is generated by illumination of the anionic equilibrated conformer R^-_{eq} we can therefore conclude that P489 is structurally related to R^-_{eq}. The small amount of P489 produced by illumination at 363.8 nm (see Figure 3C) and especially at 406.7 nm suggesting a path from RH* to P489 is explained by high-energy vibronic excitation of the anionic chromophore R^-_{eq} which overlaps with RH.

In Figure 6 we have sketched an energy potential surface extending the established energy scheme (Figure 1) which accommodates the three new low-temperature species found in this investigation. P502 and P510 can be reached directly after excitation of RH. As discussed above we actually assume that P502 and R^-_{neq} are identical species, whereas P510 is a deprotonated form distinct from P502. On the other hand P489 must be located on the energy surface close to R^-_{eq}. Since the barrier heights between the different states could be obtained only from the photoproduct side, no absolute energy position of the ground state of the photoproducts with respect to RH and R^-_{eq} can be given. The fluorescence between 420 and 470 nm associated with RH is enhanced with respect to room temperature which we attribute to the longer lifetime of RH* at low temperature.[3,4]

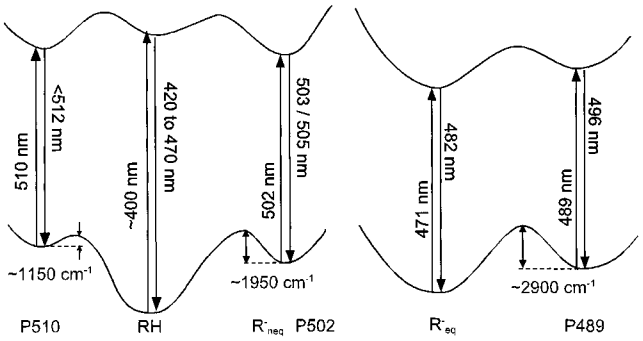

Figure 6. Extended energy potential surface of wt-GFP accommodating the three new photoproducts. The barriers are obtained from the temperature-dependent data in Figure 4.

To calculate the barriers separating the new photoproducts from the forms RH and R^-_{eq} which are stable at room-temperature we have used the temperature dependence of the fluorescence of the various photoproducts depicted in Figure 5A. As shown by Köhler and Friedrich[10] the distribution of barriers can be determined by such a heating experiment if for a given temperature T a well-defined barrier E_T exists which separates the relaxed systems from the unrelaxed. If we consider the simplest form of an activated process

$$K = K_0\, e^{\frac{-E}{k_b T}}$$

all those barriers can be crossed at a temperature T for which K^{-1} is smaller than the experimental time τ. Therefore the maximum barrier E_T which can be crossed at the temperature T is given by

$$E_T = k_b T \ln(K_0 \tau) \qquad (1)$$

As shown by Köhler and Friedrich[10] variations in τ and K_0 do not influence the results in a significant way due to the logarithmic form of the dependence.

If the heating process is stopped at a certain temperature the fluorescence intensity settles down to a quasi-steady value within a few seconds. Hence, the heating rate typically chosen for the curves shown in Figure 5A was 10 K per 70 s. If we assume for the attempt frequency (Arrhenius frequency factor) K_0 a value of 10^{12} s^{-1} the factor $\ln(K_0\,\tau)$ is about 32.

For a certain barrier distribution $f(E)$ at a given temperature T the normalized number of unrelaxed photoproducts $N(T)$ contributing to the fluorescence is given by[10]

$$N(T) = 1 - \int_0^{E_T} f(E)\mathrm{d}E \qquad (2)$$

Therefore the negative derivative of the fluorescence (which is proportional to N) with respect to T is the barrier distribution $f(E)$. The barrier distributions calculated this way are shown in Figure 5B directly below the experimental data. Obviously all three photoproducts investigated are characterized by a broad distribution of energy barriers with approximately Gaussian shape reflecting the inherent disorder of the protein. This supports the implicit assumption made above that no intermediates contribute to the observed fluorescence in the heating experiment.

Using eq 1 we can translate the temperature scale into an energy scale. Using the numbers from above the mean energy barriers for P510, P502, and P489 can be calculated as 1150, 1950, and 2900 cm^{-1}, respectively.

As mentioned above, the quantitative results are quite insensitive to the actual values of K_0 and τ. Nevertheless, to test the assumptions from above, we have recorded the fluorescence of photoproduct P510 using a much slower heating rate of 10 K per 3000 s (dotted curve in Figure 5A). Inserting this new higher value of τ into eq 1 and solving the equation for T, we calculate a shift of the maximum of the barrier distribution from 52 to 47 K. This experimentally confirms the validity of the assumptions made above.

The fact that persistent spectral holes have only be observed in the far-red wing of the absorption band of R^-_{eq} suggests a strong electron−phonon coupling of the electronic transition of wt-GFP. This also explains the difficulties in obtaining line-narrowed fluorescence spectra. Nevertheless, the absorption of R^-_{eq} has a distinct heterogeneous character as is documented by the shifts of the fluorescence spectra with excitation wavelength. In GFP the chromophore is located inside the can-like structure of the protein and therefore can act as a probe of its local, structured environment. Single molecule spectroscopy (SMS) shows inherently homogeneous lines and does not suffer from the effects of averaging as conventional ensemble spectroscopy. Low-temperature SMS studies of wt-GFP which should help to separate the various conformations and contributions to heterogeneity are under way.

These first studies at a temperature below 77 K reveal that wt-GFP shows a similar complex energy landscape as found earlier in low-temperature investigations of other proteins.[11] There are new photochemical pathways at low temperature as for example found for C-phycocyanin.[12] Each of the new products is characterized by a broad energy distribution mirroring the conformational degrees of freedom of the protein.[13] The fact stressed in the Introduction that the fluorophore is intrinsic in GFP makes this protein a very interesting candidate for further low-temperature optical high-resolution investigations of protein dynamics.

5. Conclusions

We have stabilized three new conformational states of wt-GFP at $T = 2$ K and characterized the energy surface connecting these new states with the well-established subforms at room temperature. The results indicate that the details of the photochemistry of wt-GFP are quite complex and that a variety of stable and metastable conformers and charge distributions within the protein exist. We cannot unequivocally identify the structure of the conformational states on the base of the optical investigations presented here. Future studies with various mutants of GFP as well as comparison with theoretical calculations should help clarify this question. The potential to decompose the spectral shift of the protonated chromophore into its deprotonation and reorganization components, by characterizing P502, opens exciting new perspectives for a quantitative investigation of the interaction between the chromophore and the protein matrix. The possibility of low-temperature hole burning demonstrated in this paper holds the promise of extending the single molecule room-temperature investigations of GFP to low temperature. Such investigations are already under way.

Acknowledgment. We thank G. Jung for many fruitful discussions and assistance in some experiments. We are also grateful for financial support from the DFG within SFB 377.

References and Notes

(1) Tsien, R. Y. *Annu. Rev. Biochem.* **1998**, *67*, 509.
(2) Brejc, K.; Sixma, T. K.; Kitts, P. A.; Kain, S. R.; Tsien, R. Y.; Ormö, M.; Remington, S. J. *Proc. Natl. Acad. Sci. U.S.A.* **1997**, *94*, 2306.
(3) Chattoraj, M.; King, B. A.; Bublitz, G. U.; Boxer, S. G. *Proc. Natl. Acad. Sci. U.S.A.* **1996**, *93*, 8362.
(4) Lossau, H.; Kummer, A.; Heinecke, R.; Pöllinger-Dammer, F.; Kompa, C.; Bieser, G.; Jonsson, T.; Silva, C. M.; Yang, M. M.; Youvan, D. C.; Michel-Beyerle, M. E. *Chem. Phys.* **1996**, *213*, 1.
(5) Calfie, M.; Tu, Y.; Euskirchen, G.; Ward, W. W.; Prasher, D. *Science* **1994**, *263*, 802.
(6) Gredes, H. H.; Kaether C. *FEBS Lett.* **1996**, *389*, 44.
(7) Dickson, R. M.; Cubitt, A. B.; Tsien, R. Y.; Moerner W. E. *Nature* **1997**, *388*, 355.
(8) Jung, G.; Wiehler, J.; Göhde, W.; Tittel, J.; Basché, T.; Steipe, B.; Bräuchle, C. *Bioimaging* **1998**, *6*, 54.
(9) Skinner, J. L.; Moerner, W. E. *J. Phys. Chem.* **1996**, *100*, 13251.
(10) Köhler, W.; Friedrich, J. *Phys. Rev. Lett.* **1987**, *59*, 2199.
(11) Parak, F.; Frauenfelder, H. *Physica A* **1993**, *201*, 332.
(12) Friedrich, J.; Scheer, H.; Zickendraht-Wendelstadt, B.; Haarer, D. *J. Am. Chem. Soc.* **1981**, *103*, 1030.
(13) Leeson, D. T.; Wiersma, D. A.; Fritsch, K.; Friedrich, J. *J. Phys. Chem. B* **1997**, *101*, 6331.